Les Cahiers du GERAD ISSN: 0711–2440

Contingency-type reserve leveraged through aggregated thermostatically-controlled loads – Part II: Case studies

A. Abiri Jahromi
F. Bouffard

G–2014–90

November 2014

GERAD HEC Montréal
3000, chemin de la Côte-Sainte-Catherine
Montréal (Québec) Canada H3T 2A7

Tél. : 514 340-6053
Téléc. : 514 340-5665
info@gerad.ca
www.gerad.ca

Contingency-type reserve leveraged through aggregated thermostatically-controlled loads – Part II: Case studies

Amir Abiri Jahromi
François Bouffard

GERAD & Department of Electrical and Computer Engineering, McGill University, Montréal (Québec) Canada, H3A 0E9

amir.abiri-jahromi@mail.mcgill.ca
francois.bouffard@mcgill.ca

November 2014

Les Cahiers du GERAD

G–2014–90

Abstract: An analytical approach and a control strategy are proposed in Part I of this two-part paper for leveraging the aggregate demand of a population of Thermostatically-Controlled Loads (TCLs) to deliver contingency-type reserve capacity. Further, a metric is introduced to quantify the TCL users' comfort satisfaction in response to a control signal. In Part II, we address the validation of the concepts put forth in the first part of the paper. To do so, we develop an extensive set of case studies based upon a population of 10 000 electric water heaters (EWH). Here, a physically-based model is first derived for the calculation of EWHs on-time statistics. The model is then extended to calculate the probability of EWH users' comfort satisfaction. The analytical approach and control strategy presented in Part I are validated using the EWH model against Monte Carlo simulations. Further, the trade-off between demand response capacity and EWH users' comfort satisfaction is investigated.

Key Words: Aggregate demand response capacity, electric water heaters, user comfort, sensitivity analysis.

Acknowledgments: This work was supported in part by the Natural Sciences and Engineering Research Council of Canada, Ottawa (Ontario) Canada.

Nomenclature

The main symbols used in the paper are listed here for the convenience of the reader.

$f_{L_d}(\ell_d)$	Probability distribution of hot water drawage from EWH
$f_{T_T}(t_T)$	Probability distribution of hot water temperature inside EWH tank
L_d	Random variable denoting volume of hot water drawage from EWH
L_d^{min}, L_d^{max}	Minimum and maximum volume of hot water drawage from EWH
L_d^*	Minimum volume of hot water drawage resulting in EWH operation
L_d^{**}	Maximum volume of hot water drawage not violating user's comfort
P_r	Rated power of EWH heating element
$P(OFF)$	Probability of EWH in off-state
$P(ON)$	Probability of EWH in on-state
$P(ON\|T \geq T_0)$	Probability of EWH in on-state satisfying users' comfort
$P(ON\|T < T_0)$	Probability of EWH in on-state not satisfying users' comfort
t_{min}	EWH minimum on-time
t_{max}	EWH maximum on-time
T_{th}^{min}	EWH minimum thermostat deadband
T_{th}^{max}	EWH maximum thermostat deadband
T_T	Random variable denoting temperature inside EWH tank
T_{in}	Temperature of inlet water to EWH
T_{on}	On-time of EWH in a normal on-off cycle
T_{on}^R	On-time of EWH required to satisfy user comfort
T_{on}^{min}	Controllable minimum on-time of EWH
T_0	EWH users' comfort threshold for hot water temperature
V	Volume of EWH tank
$Y]$	Probability distribution of EWHs on-time
c	Specific heat capacity of water
ρ	Density of water

1 Introduction

A general analytical approach and a control strategy are proposed in Part I [1] of this two-part paper for leveraging the statistical bounds on the exploitable flexibility from a population of N TCLs as a contingency-type reserve resource. This characterization is underpinned by the control behavior of individual TCLs in response to an activation signal.

This second part presents an application of the proposed analytical approach from Part I to a population of $N = 10\,000$ electric water heaters (EWH) whose consumption flexibility is used to provide reserve capacity. The objective here is to demonstrate that the analytical characterization approach, which is based on population statistics only, is appropriate to estimate the expected response of the population and its uncertainty bounds. At the same time, this should provide good evidence about how an aggregator could use individual TCL controller parameters to obtain desired aggregate reserve capacity volume, uncertainty and reconnection behavior, while ensuring TCL users' comfort satisfaction.

The remainder of this part is organized as follows. A physically-based model is derived in Section 2 for the calculation of individual EWH on-time statistics based on typical EWH parameters and hot water drawage probability distributions. The necessary analytics for the calculation of the probability of EWH users' comfort satisfaction are derived in Section 3. In Section 4, Monte Carlo simulations are employed to validate the numerical results obtained by the proposed analytical approach for a population of 10 000 EWHs. In addition, the trade-off between demand response capacity and EWH users' comfort satisfaction is investigated through several case studies. Finally, the conclusions of the paper are presented in Section 5.

2 A physically-based model for the calculation of EWH on-time statistics

A basic EWH consists of a storage tank, a thermostat, a heating element, an inlet (cold) water pipe and a hot water outlet pipe [2].

To determine the minimum and maximum on-time of a typical EWH, t_{min} and t_{max}, and the probability distribution of EWH on-time, Y, we have to model its energy flows. The drivers for energy flows are: 1) hot water usage followed by its replacement by cold water, and 2) wall conduction losses. The first driver is the dominating one because the time constants for energy flows via wall conduction are much longer. When a EWH does have to turn on, its minimum on-time (t_{min}) is associated with the tank water temperature having dropped below the minimum thermostat deadband, T_{th}^{min}, without water drawage. This event activates the heating element until the water temperature rises to the maximum thermostat deadband setting, T_{th}^{max}. Therefore,

$$t_{min} = \frac{c\rho V(T_{th}^{max} - T_{th}^{min})}{P_r} \tag{1}$$

where c and ρ denote the specific heat and density of water, respectively, V is the tank volume and P_r is the rated power of the heating element. The maximum on-time (t_{max}), on the other hand, occurs when the tank water temperature drops below the minimum thermostat deadband concurrently with maximum hot water drawage

$$t_{max} = t_{min} + \frac{c\rho L_d^{max}(T_{th}^{min} - T_{in})}{P_r} \tag{2}$$

where, L_d^{max} is the maximum value for hot water drawage, and T_{in} is the inlet water temperature. This result can be interpreted as the time to heat up to T_{th}^{min} a volume of L_d^{max} liters from an initial temperature of T_{in} followed by further heating time of t_{min} to bring the tank water volume up to T_{th}^{max}.

The EWH on-time random variable Y is a function of two other random variables, namely T_T and L_d. Here T_T is the water temperature measured by the thermostat when drawage starts. L_d is the total volume of water drawn, which accounts for water drawn continuously before the EWH turns on and for water drawn while the EWH is on. From this, Y takes the form

$$Y = g(T_T, L_d) = \frac{c\rho V(T_{th}^{max} - T_T)}{P_r} + \frac{c\rho L_d(T_T - T_{in})}{P_r} \tag{3}$$

In a way similar to (2), Y accounts for the need to bring up the entire volume of water from T_T to T_{th}^{max} (first term) and the drawn amount from T_{in} up to T_T (second term).

In the absence of water drawage, the water temperature is assumed to be a uniform random variable ranging between the EWH thermostat deadband settings.

$$f_{T_T}(t_T) = \frac{1}{T_{th}^{max} - T_{th}^{min}} \tag{4}$$

It is noteworthy that this modeling assumption results in the most conservative scenario in terms of uncertainty. Obviously, using more accurate distributions (due to having temperature sensing information, for example) will result in more accurate and less conservative scenarios.

As for L_d, unlike the approaches of [2] and [3], we recall that this amount is a total volume of water drawn and not a rate of drawage (in liters per minute, for example). Therefore, the typical Markov models for hot water consumption are not appropriate here. Instead, for the sake of this study, we assume that L_d is beta-distributed for the following two main reasons. First, the beta distribution is bounded, which is the case for hot water consumption, *i.e.*, L_d^{min}, L_d^{max}. Second, because it has shape parameters p and q, the distribution can be adjusted to capture randomness that displays both skew and kurtosis [4]. Therefore,

$$f_{L_d}(\ell_d) = \frac{\Gamma(p+q)}{\Gamma(p)+\Gamma(q)} \frac{(\ell_d - L_d^{min})^{(p-1)}(L_d^{max} - \ell_d)^{(q-1)}}{(L_d^{max} - L_d^{min})^{(p+q-1)}} \tag{5}$$

where $\Gamma(\cdot)$ is the gamma function.

We assume that T_T and L_d are not correlated at the beginning of a water drawage interval. Further, it is important to recognize that there is a minimum volume of water drawage over which the EWH turns on because it brings the overall EWH water temperature below T_{th}^{min}. This volume of water, L_d^*, is such that $(V - L_d^*)(T_T - T_{th}^{min}) = L_d^*(T_T - T_{in})$, which implies that

$$Y = \begin{cases} 0, & \text{if } L_d < L_d^* \\ g(T_T, L_d), & \text{otherwise} \end{cases} \tag{6}$$

where $L_d^* = V(T_T - T_{th}^{min})/(T_T - T_{in}) \geq 0$ depends on the realization of T_T at the beginning of the drawage period. We note that in the case where $L_d = 0$ and the water temperature drops to T_{th}^{min}, (6) sets the EWH on-time to t_{min}.

We can thus infer the conditional cumulative distribution function of Y from those of T_T and L_d

$$F_Y(y|t_T, \ell_d) = F_{L_d}\left(\frac{V(t_T - T_{th}^{min})}{t_T - T_{in}}\right) \cdot \left[1 - F_{T_T}\left(\frac{VT_{th}^{min} - \ell_d T_{in}}{V - \ell_d}\right)\right], \text{ if } 0 \leq y < t_{min} \tag{7}$$

$$F_Y(y|t_T, \ell_d) = \left[1 - F_{L_d}\left(\frac{V(t_T - T_{th}^{min})}{t_T - T_{in}}\right)\right] \cdot F_{T_T}\left(\frac{VT_{th}^{min} - \ell_d T_{in}}{V - \ell_d}\right), \text{ if } t_{min} \leq y \leq t_{max}. \tag{8}$$

The probability distribution function of Y can be obtained from these to compute its mean and variance (Part I, Appendix A [1]). It is noteworthy that demand flexibility aggregators could resort to laboratory data collection and analysis or to smart metering data from which EWH on-time information has been extracted from (see, for instance, [5]) on a large enough EWH population sample to obtain the same success in evaluating Y statistics for different hours and times of the year.

3 Probability of EWH users' comfort satisfaction

In Part I, we introduced a metric, C, to quantify the trade-off between demand response capacity and TCL users' comfort satisfaction probability

$$C = \frac{P(ON|T \geq T_0)}{P(ON)} \tag{9}$$

This metric requires the calculation of the probabilities that the participating EWHs are in the on-state, given that the users' comfort is satisfied. Moreover, we shall use the fact that

$$\begin{aligned} P(ON|T \geq T_0) &= 1 - P(OFF) - P(ON|T < T_0) \\ &= P(ON) - P(ON|T < T_0) \end{aligned} \tag{10}$$

In the following subsections, we use the physically-based model from Section 2 to calculate those probabilities.

3.1 Probability of EWHs in the on- and off-states

In the previous section, it is shown that for each temperature within the EWH control deadband, $T_{th}^{min} \leq T_T \leq T_{th}^{max}$, there is a minimum volume of hot water drawage, L_d^*, over which the EWH turns on because it brings the overall EWH temperature below T_{th}^{min}. This means that the bounds on L_d^* are

$$0 \leq L_d^* \leq \frac{V(T_{th}^{max} - T_{th}^{min})}{(T_{th}^{max} - T_{in})} = L_d^{*,max} \tag{11}$$

In addition, for each volume of hot water drawage, L_d, there is a minimum tank temperature within the EWH deadband settings, T_T^*, for which the EWH would not operate. This is so because this drawage volume cannot bring the overall water temperature below T_{th}^{min}

$$T_T^* = \frac{VT_{th}^{min} - T_{in}L_d}{(V - L_d)} \tag{12}$$

Thus, from (11) and (12), we can find the probability of EWHs being in the off-state

$$P(OFF) = F_{L_d,T_T}\left(L_d^{*,max}, T_{th}^{max}\right) - F_{L_d,T_T}\left(L_d^{*,max}, T_T^{*}\right) \tag{13}$$

The first term in (13) is interpreted as the probability of EWHs in the population with water drawage volume under $L_d^{*,max}$ and with temperatures under T_{th}^{max}. The second term is interpreted as the probability of EWHs in the population with water drawage volume under $L_d^{*,max}$ and inside tank temperature under T_T^* (*i.e.*, EWHs with hot water drawage volume under $L_d^{*,max}$ which have to turn-on). From this, we find the probability of EWHs in the on-state

$$P(ON) = 1 - P(OFF) \tag{14}$$

In (13) and (14), we assume that the upper bound of L_d^* is less than the maximum volume of hot water drawage, *i.e.*, L_d^{max}. Otherwise, the bound, $L_d^{*,max}$, should be replaced by L_d^{max}.

3.2 Probability of EWHs in the on-state not satisfying users' comfort

The EWH on-time, T_{on}^R, required to satisfy an arbitrary EWH user comfort level, $T_0 \leq T_{th}^{min}$, is calculated as

$$T_{on}^R = \frac{c\rho V(T_0 - T_T) + c\rho L_d(T_T - T_{in})}{P_r} \tag{15}$$

Further, the EWH on-time, T_{on}, in a normal cycle (not disturbed by a control signal) is calculated as

$$T_{on} = \frac{c\rho V(T_{th}^{max} - T_T) + c\rho L_d(T_T - T_{in})}{P_r} \tag{16}$$

From (15) and (16) it can be inferred that EWHs responding to a demand response activation signal satisfy or dissatisfy their users' comfort respectively by the probabilities of $(1 - T_{on}^R/T_{on})$ and (T_{on}^R/T_{on}) regardless of the choice of the control parameter T_{on}^{min}. This is because an EWH could be at any point within its on-cycle, when a demand response activation signal is broadcasted, with equal probability.

Moreover, for each choice of the control parameter T_{on}^{min} and tank temperature T_T, there is a maximum volume of water drawage, L_d^{**}, that will not violate the users' minimal comfort level T_0

$$L_d^{**} = \frac{c\rho V(T_T - T_0) + P_r T_{on}^{min}}{c\rho(T_T - T_{in})} \tag{17}$$

Also, the bounds on L_d^{**} are

$$L_d^{**,min} = \frac{c\rho V(T_{th}^{min} - T_0) + P_r T_{on}^{min}}{c\rho(T_{th}^{min} - T_{in})} \tag{18}$$

$$L_d^{**,max} = \frac{c\rho V(T_{th}^{max} - T_0) + P_r T_{on}^{min}}{c\rho(T_{th}^{max} - T_{in})} \tag{19}$$

Furthermore, for each choice of T_{on}^{min} and water drawage volume L_d, there is a minimum tank temperature within the EWH deadband, T_T^{**}, for which the users' comfort level T_0 will not be violated

$$T_T^{**} = \frac{c\rho V T_0 - c\rho T_{in} L_d - P_r T_{on}^{min}}{c\rho(V - L_d)} \tag{20}$$

From (17)–(20), we have the bounds on the random variables T_T and L_d for EWHs in the on-state that do not satisfy users' comfort through operation for T_{on}^{min} minutes. The probability of this random event is

$$P(ON|T < T_0) = \int_{L_d^1}^{L_d^2}\int_{T_T^1}^{T_T^2}\left(\frac{T_{on}^R}{T_{on}}\right) f_{L_d}(\ell_d) f_{T_T}(t_T)\, dt_T\, d\ell_d + \int_{L_d^3}^{L_d^4}\int_{T_T^3}^{T_T^4}\left(\frac{T_{on}^R}{T_{on}}\right) f_{L_d}(\ell_d) f_{T_T}(t_T)\, dt_T\, d\ell_d \tag{21}$$

where the integration limits are given by

$$\begin{cases} L_d^1 = L_d^{**,min}, & L_d^2 = L_d^{**,max} \\ T_T^1 = T_{th}^{min}, & T_T^2 = T_T^{**} \end{cases}$$

and

$$\begin{cases} L_d^3 = L_d^{**,max}, & L_d^4 = L_d^{max} \\ T_T^3 = T_{th}^{min}, & T_T^4 = T_{th}^{max} \end{cases}$$

The first term in (21) is the probability of EWHs with water drawage volume between $L_d^{**,min}$ and $L_d^{**,max}$ that do not satisfy users' comfort as their T_T is less than T_T^{**}. The second term is interpreted as the probability of EWHs with water drawage volume beyond $L_d^{**,max}$. The EWHs with water drawage volume over $L_d^{**,max}$ cannot satisfy their users' comfort for any tank temperature within the deadband.

From the analytics developed in this section, one can calculate the optimal value for the control parameter, T_{on}^{min}, to guarantee the requested level of EWH users' comfort, T_0, for a prescribed value of the metric C.

4 Numerical studies

The physically-based model and analytics derived in the previous sections are employed here to validate the proposed analytical approach and the control strategy presented in Part I of the paper for a population of 10 000 EWHs.

4.1 Characterizing the bounds on exploitable flexibility from a population of EWHs

4.1.1 Analytical approach

The analytical approach presented in Part I is employed to characterize the statistics on the flexibility that is exploitable from the 10 000 EWH population. As shown in Part I (Section III), the flexibility exploitable from a TCL population depends on the mean value of individual TCLs random variable Y_i which is calculated in (22) considering the parameters given in Tables 4 and 5 of Appendix A.

$$\mu_y = \int_0^{t_{max}} y f_{Y_i}(y)\, dy = 0.2077. \tag{22}$$

Thus, the mean μ_d and the standard deviation σ_d parameters of any $D_i(X_i, Y_i)$ are respectively 0.2077 and 0.4056 per unit (as shown in Appendix A of Part I). Further, according to the analytics derived in Part I (Section 3), the 90% confidence coefficient bounds on the flexibility achievable from this population are calculated in (23) for the hot water drawage probability distribution in Table 5 and the EWH parameters in Table 4 of Appendix A.

$$P\{2077 - \nu_{90\%}40.56 < A_d < 2077 + \nu_{90\%}40.56\} = 0.9. \tag{23}$$

From this, we find that $2010 \leq A_d \leq 2144$ with 90% certainty. Otherwise said, 90% of the time, between 2010 and 2144 EWHs out of the 10 000 in the population will respond to demand response activation signal.

4.1.2 Monte Carlo simulation

In this section, we validate the analytical flexibility characterization approach by conducting a randomization experiment to obtain A_d and its statistics by simulation. Here, the temperature inside the tank and the hot water drawage are randomly drawn from the same uniform and beta distributions used in the analytical approach (with the parameters given in Tables 4 and 5 of the Appendix A).

The flexibility achievable from 10 000 EWHs is found from 10 000 Monte Carlo simulations, and the results are plotted in Figure 1. The per-unit mean (μ_d) and standard deviation (σ_d) of the Monte Carlo simulations are 0.2067 and 0.4049 respectively. These values are consistent with the analytical results obtained previously

(μ_d here is within 0.48% of the value found in Section 4.1.1 and σ_d is within 0.17% of the analytically-found value).

The 90% confidence interval and the three standard deviation boundaries obtained from the analytical approach are shown by solid and dashed lines respectively in Figure 1 to show their close agreement with the simulation experiment. It is noteworthy that according to the well-known rule of thumb for normal distributions [6], roughly 99.7% of the samples should lie within three standard deviations from the mean since the aggregated response should have a normal distribution by the Central Limit Theorem.

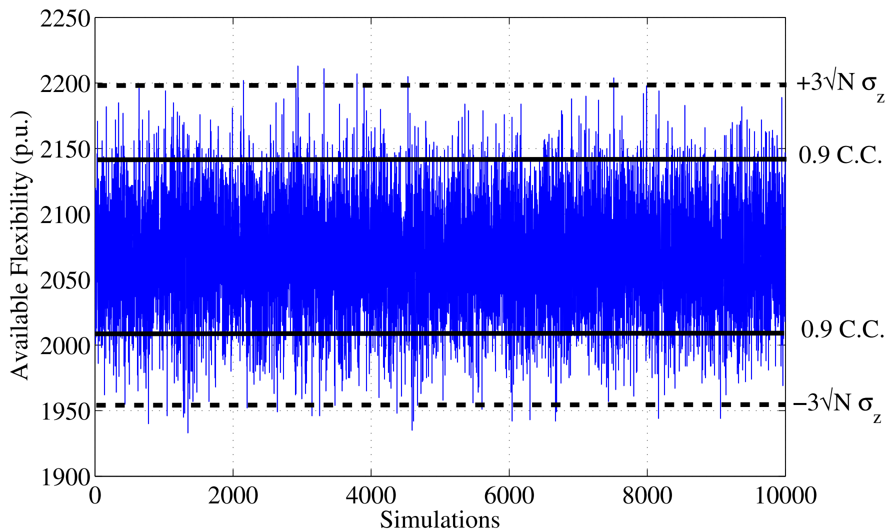

Figure 1: Representation of 10 000 Monte Carlo simulations characterizing the achievable flexibility from 10 000 EWHs

4.2 Controlling the statistical bounds of the EWHs response and their reconnection

4.2.1 Analytical approach

As discussed in Part I (Section 4), the response level of the population of TCLs is controllable by adjusting the parameter T_{on}^{min}. Further, the number of EWHs reconnecting to grid at each instant of time is controllable by adjusting the parameter $T_{reconnect}$ while considering the response bounds. The aggregated response level of EWHs for three different values of parameter T_{on}^{min}, *i.e.*, 10 minutes, 20 minutes and 25 minutes, are calculated using the analytical approach and summarized in Table 1.

In addition, the rate of EWH reconnection to the grid at each instant of time, $S_{reconnect}$, is calculated here for two different values of the parameter $T_{reconnect}$, *i.e.*, 25 minutes and 30 minutes. The parameter $T_{reconnect}$ consists of the fixed parameter T_{off}^{min}, which here equals 20 minutes, and the random time delay parameter T_{delay}^{random} distributed uniformly between $T_1 = 0$ and to either $T_2 = 5$ or 10 minutes respectively. We recall that T_{off}^{min} ensures that the duration of the response is minimally sustained, while the difference $T_2 - T_1$ determines the number of EWHs reconnecting to the grid at each instant of time. The results, from the analytical calculations, are summarized in Table 2.

Table 1: 90% statistical bounds on aggregated response of 10 000 EWHs for different values of T_{on}^{min}

T_{on}^{min} (min)	$N\mu_r$ (p.u.)	$\sqrt{N}\sigma_r$ (p.u.)	90% A_r (p.u.)
10	1542	36.1	(1483, 1602)
20	1008	30.1	(959, 1058)
25	740	26.2	(698, 784)

Table 2: 90% statistical bounds on the number of EWHs reconnecting to the grid

$T_2 - T_1$ (min)	T_{on}^{min} (min)	$N\mu_r$ (p.u.)	$\sqrt{N}\sigma_r$ (p.u.)	90% $S_{reconnect}$ (p.u./min)
5	10	1542	36.1	(297, 321)
	20	1008	30.1	(192, 212)
	25	740	26.2	(140, 157)
10	10	1542	36.1	(149, 161)
	20	1008	30.1	(96, 106)
	25	740	26.2	(70, 79)

4.2.2 Monte Carlo simulations

Figure 2 illustrates the Monte Carlo simulation results for the previously used three values of T_{on}^{min}, (10 , 20 and 25 minutes). As expected, it can be seen from Figure 2 that the aggregated response is reduced by increasing the parameter T_{on}^{min}. It is also noteworthy that the uncertainty associated with the response reduced accordingly by increasing that parameter. This is because the number of potentially responding EWHs is reduced as they are forced to remain on if an activation signal is received. On visual inspection, the Monte Carlo simulation results obtained here are consistent with the numbers obtained by the analytical approach.

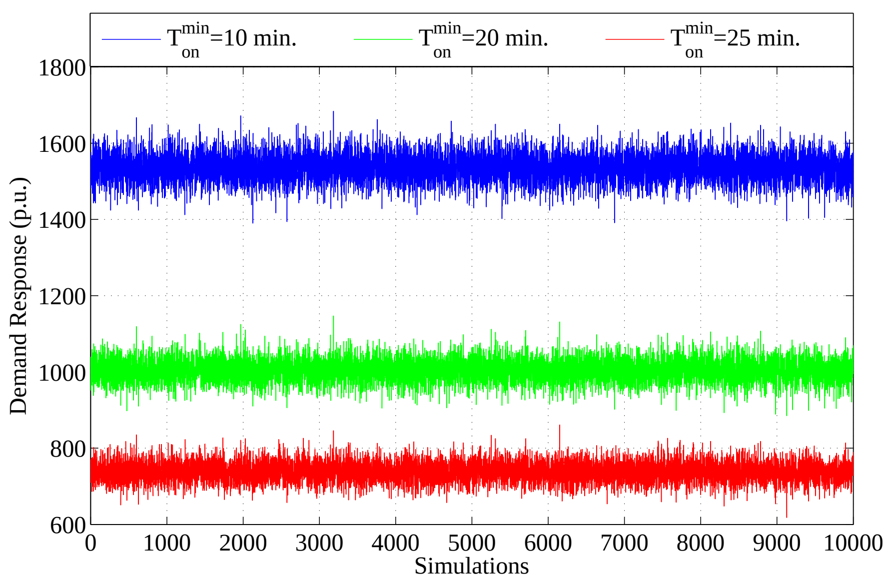

Figure 2: Representation of 10 000 Monte Carlo simulations indicating the controllability of the response level of 10 000 EWHs using parameter T_{on}^{min}

In addition, the EWHs reconnection to the grid is replicated using Monte Carlo simulation for T_{delay}^{random} uniformly distributed between $T_1 = 0$ and $T_2 = 5$ minutes as shown in Figure 3. As it can be seen, the rate at which EWH reconnect to grid is controllable by the range of $T_2 - T_1$.

4.3 Employing EWHs for primary frequency control

In this section, we apply the analytical characterization technique and the control of a TCL population for the provision of reserve capacity for primary frequency control. In this case, the aggregator activation signal is the grid frequency error measured by each TCL combined with aggregator-assigned cutoff frequency error thresholds. In other words, each TCL measures the grid frequency and compares it to its reference and

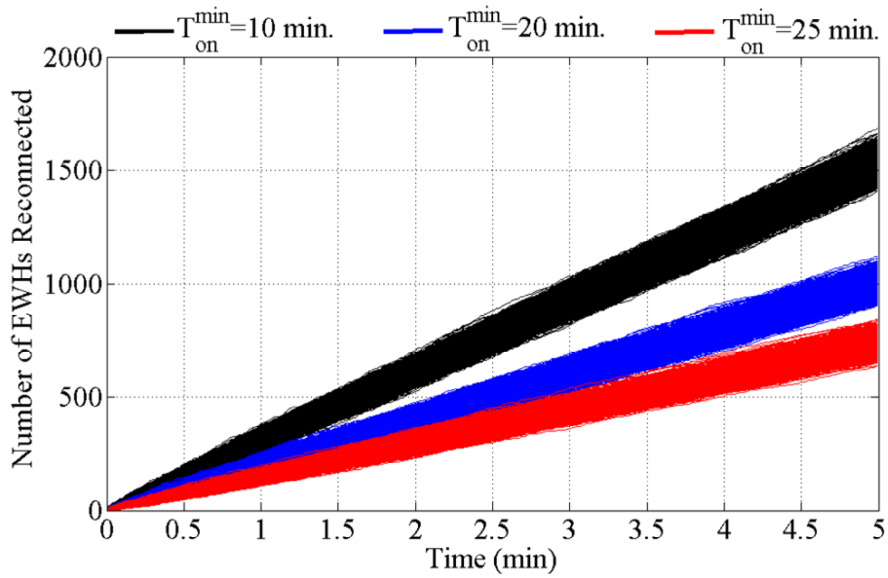

Figure 3: Representation of 10 000 Monte Carlo simulations for the EWHs reconnection to grid when $T_{delay}^{random} = 5$ minutes

responds if the error is over aggregator-assigned threshold, in a way similar to what is described in [7,8]. By having an even share of the TCL population per discrete frequency threshold, the population should be able to emulate a droop characteristic.

In this case study, we assume that the cutoff frequency error thresholds of 10 000 EWHs are uniformly distributed between frequencies of 58.5 Hz to 59.5 Hz with equal spacing of 0.01 Hz (thus allocating 100 EWHs per 0.01 Hz frequency band). Moreover, to assess the impact of T_{on}^{min} on the population response, T_{on}^{min} is varied in five minute increments from 0 to 25 minutes to show that the aggregated response of EWHs emulates a droop characteristic similar to that of conventional generating units with governor control.

4.3.1 Analytical approach

The statistics μ_r, σ_r, the 90% confidence coefficient statistical bounds on the EWH population response over the frequency range of 58.5 Hz to 59.5 Hz, the mean droop and droop three sigma bounds are summarized in Table 3. Note that the bounds on A_r provided in Table 3 represent the number of EWHs responding to grid frequency errors at each of the 0.01 Hz frequency steps between 58.5 to 59.5 Hz as EWH population power is normalized.

It can be seen from Table 3 that the number of EWHs responding to frequency errors is reduced by increasing parameter T_{on}^{min} from 0 to 25 minutes. It is noteworthy that the uncertainty associated with the cumulative response of EWHs increases from frequency 59.5 Hz to 58.5 Hz by the factor of 10. This is

Table 3: 90% Statistical bounds on aggregated response of 10 000 EWHs participating in primary frequency control

T_{on}^{min} (min)	$N\mu_r$ (p.u.)	$\sqrt{N}\sigma_r$ (p.u.)	90% A_r (p.u./0.01 Hz)	Mean droop (p.u./Hz)	$3\sigma_r$ droop (p.u./Hz)
0	2077	40.6	(14, 28)	2077	± 122
5	1809	38.5	(12, 25)	1809	± 116
10	1542	36.1	(10, 22)	1542	± 109
15	1275	33.4	(7, 18)	1275	± 101
20	1008	30.1	(5, 15)	1008	± 91
25	740	26.2	(3, 12)	740	± 79

because, the uncertainty is proportional to $\sqrt{N}\sigma_r$ and the number of EWHs participating in frequency control increases from 100 to 10 000 over the frequency range 59.5 Hz to 58.5 Hz. It can also be seen from Table 3 that the droop and droop 3σ bounds, which respectively indicate the average number of EWHs responding to frequency errors when the frequency drops to 58.5 Hz and the corresponding 3σ bounds, reduces by increasing T_{on}^{min}.

4.3.2 Monte Carlo simulations

As it can be seen in Figure 4, the EWH population emulates a droop characteristics similar to the conventional generating units whose slope is controllable by parameter T_{on}^{min}. The first difference between the droop characteristics of a conventional generating unit and a TCL-based resource is that the droop in the former one is defined by a fixed value while the droop in the latter is a range as summarized in Table 3. Second, the duration that the response can be sustained by a TCL-based resource is defined by the parameter T_{off}^{min} which depends on EWH users' comfort level that has to be satisfied. The simulation results are confirming the analytical estimations found in Table 3.

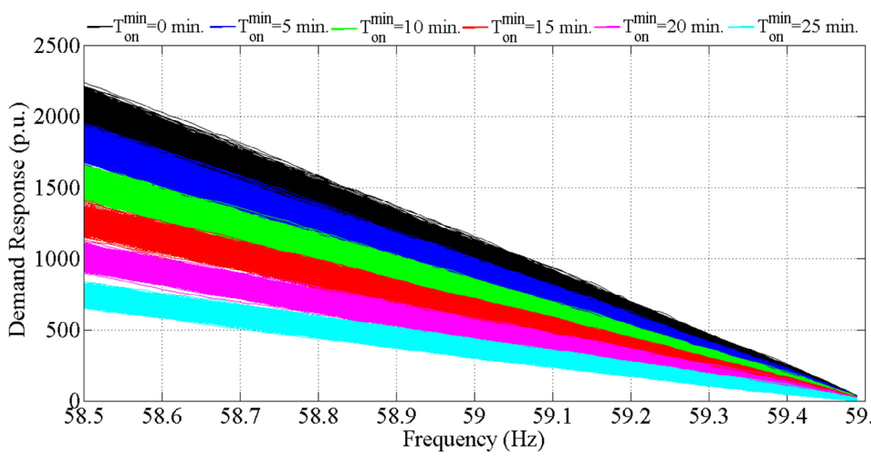

Figure 4: Representation of 10 000 Monte Carlo simulations for the cumulative response of 10 000 EWHs which are uniformly distributed over the frequency range of 59.5 Hz to 58.5 Hz with different values of T_{on}^{min}

4.4 Trade-off between EWH Users' comfort satisfaction and demand response capacity

In this section, the trade-off between EWH users' comfort satisfaction and demand response capacity is examined. Further, the available demand response capacity is assessed against the influence of factors such as inlet water temperature, hot water usage patterns and EWH users' comfort threshold.

4.4.1 Study 1

In this study, the trade-off between demand response capacity and comfort satisfaction is examined for the hot water drawage probability distribution in Table 5 and the EWH parameters in Table 4, Appendix A. The comfort threshold T_0 is assumed to be equal to the EWH minimum thermostat deadband, *i.e.*, 115°F. The metric C is calculated to be 84.9%. This indicates that 84.9% of responsive users had their comfort level satisfied during demand response calls. In this case, the statistical bounds on the exploitable flexibility from the 10 000 EWHs are between 2010 and 2144 per unit with 90% confidence coefficient.

Next, the control parameter T_{min}^{on} is calculated such that the metric C is increased to 95%. This criterion is satisfied by setting the control parameter T_{min}^{on} to 11.5 minutes. Yet, by letting T_{min}^{on} equal 11.5 minutes, the statistical bounds on the demand response capacity stand between 1403 and 1520 per unit with 90% confidence coefficient. Thus, increasing T_{min}^{on} from zero to 11.5 minutes increased the metric C by 11.9% and decreased the demand response capacity approximately by 29.6%. This study indicates that the EWH users' comfort plays an important role in determining the available demand response capacity for different types of reserves provided by EWHs.

For instance, we argue that aggregators can exploit all the achievable demand response capacity from 10 000 EWHs for sporadic applications such as contingency reserve as their deployment is rather infrequent, while approximately 85% of EWH users would always be satisfied with their quality of service. It is also noteworthy that the remaining 15% of EWH users that are not satisfied with their quality of service would not be the same at different events since the users usage pattern and response are stochastic. The same argument may not be valid in the case of continuous applications such as regulation, as the control is expected to happen continuously. In such cases, aggregators may need to increase the probability of EWH users' comfort satisfaction to 95% or even more to avoid response fatigue.

Now, we assume that EWH users agree to degrade their comfort threshold by 2°F under the EWH minimum thermostat deadband setting, *i.e.*, $T_0 = 113°\text{F}$. The parameter T^{on}_{min} is recalculated such that the metric C remains at 95%. In this case, T^{on}_{min} has to be equal to 6.6 minutes. Further, the statistical bounds on demand response capacity now stand between 1661 and 1786 per unit with 90% confidence coefficient. This analysis indicates that lowering the EWH users' comfort threshold may have significant impact on the available demand response capacity. Here, by degrading the EWH users' comfort by 2°F only, the available demand response capacity increased by 17.9%.

4.4.2 Study 2

In this study, the trade-off between demand response capacity and EWH users' satisfaction is further investigated by considering daily hot water usage patterns. The impact of influencing factors such as inlet water temperature and EWH users' comfort threshold are also assessed.

Two inlet water temperatures, 1.5°C and 23°C, are considered respectively representing a typical extreme winter low temperature and a typical extreme summer high temperature. Further, the shape parameters of the beta distribution, p and q, are employed to capture the variations of the hourly hot water usage pattern between the minimum and maximum usage values (Appendix A, Table 6). The 90% confidence bounds on the exploitable flexibility and the metric C are first calculated over the daily horizon without controlling the EWH users' comfort, as shown in Figures 5 and 6. As it can be seen, available demand response capacity and responsive EWH users' comfort varies significantly over a daily cycle. This is due to the variations in the hot water usage pattern. Further, a significant difference between the available demand response potential and EWH users' comfort satisfaction can be observed in the summer and winter, which is due to the differences in inlet water temperatures. These variations emphasize the need to analyze the trade-off between the available capacity for different types of reserves and EWH users' comfort satisfaction. Further, it can be seen from Figure 6, that a 95% comfort satisfaction criterion is satisfied without the need for control at several hours when low hot water usage is common. This is an important observation since it indicates that EWH users' comfort is at higher risk in the hours with higher levels of usage and demand response potential. This emphasizes the need to define correctly the EWH users' comfort threshold while deploying EWHs demand response for different types of reserves.

Next, T^{on}_{min} is calculated such that the metric C is increased to at least 95% in all hours of the day. The T^{on}_{min} parameters obtained for different hours are plotted in Figure 7. Further, the 90% confidence bounds on demand response capacity and the metric C are recalculated and plotted in Figures 8 and 9. By comparing Figures 5 and 8, it can be seen that the difference between the available demand response potential in the summer and winter are decreased by bounding the EWH users' comfort. This is expectable since the higher demand response potential in the winter stems from the lower inlet water temperature, and the need for longer on-time.

Next, we examine the impact of the EWH users' comfort threshold on the available demand response capacity. The EWH users' comfort threshold is again reduced by 2°F and T^{on}_{min} is recalculated such that 95% EWH users' comfort is satisfied. The values for T^{on}_{min} are plotted in Figure 10. The 90% confidence bounds on the demand response capacity and the metric C are also recalculated and plotted in Figures 11 and 12. By

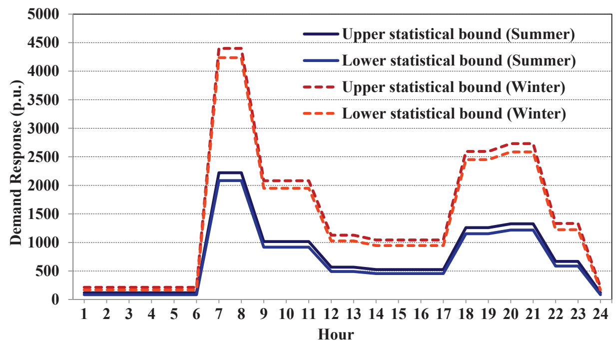

Figure 5: 90% confidence bounds on hourly demand response capacity from 10 000 EWHs in typical summer and winter days ($T_0 = 115°$F)

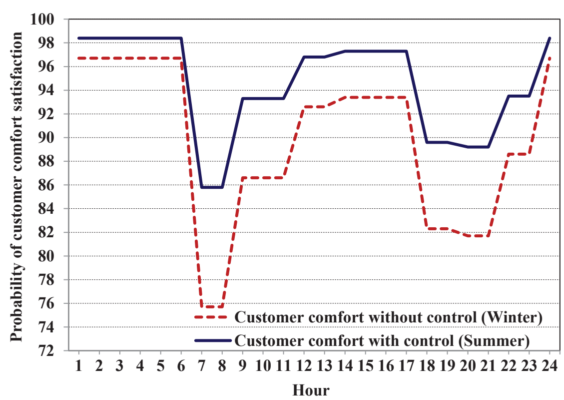

Figure 6: Metric C in typical summer and winter days ($T_0 = 115°$F)

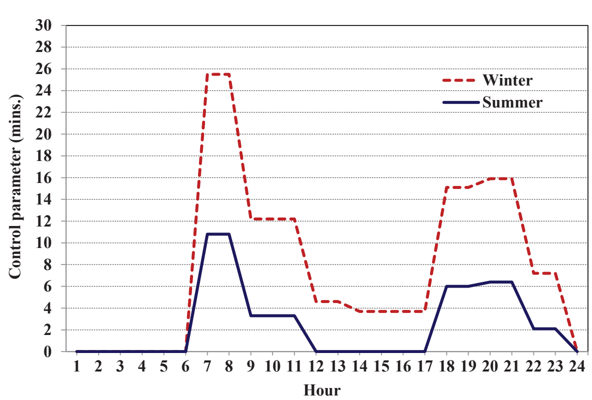

Figure 7: The control parameter T_{min}^{on} necessary to maintain EWH users' comfort index of 95% ($T_0 = 115°$F)

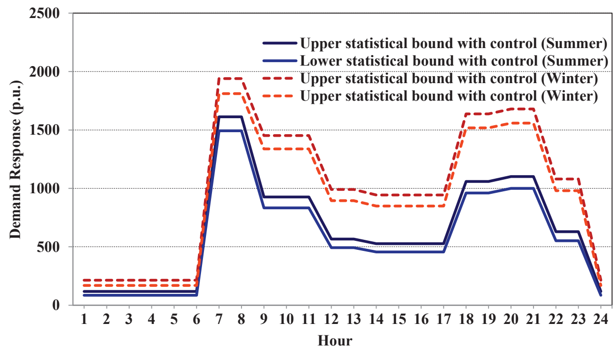

Figure 8: 90% confidence bounds on hourly demand response capacity from 10 000 EWHs with control over users comfort in typical summer and winter days ($T_0 = 115°\mathrm{F}$)

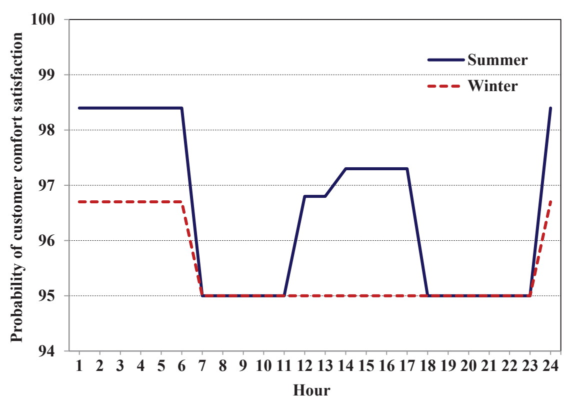

Figure 9: Metric C with control over users' comfort ($T_0 = 115°\mathrm{F}$)

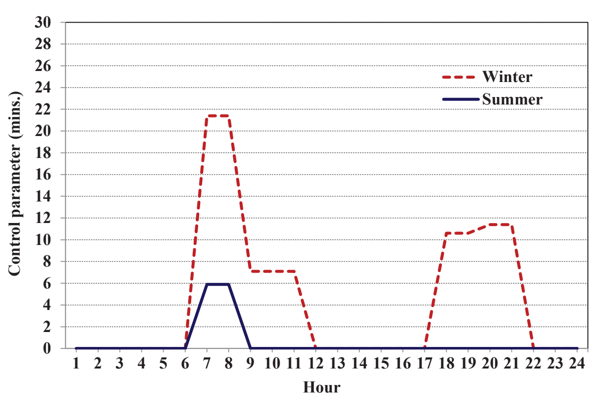

Figure 10: The control parameter T_{min}^{on} necessary to maintain EWH users comfort index of 95% ($T_0 = 113°\mathrm{F}$)

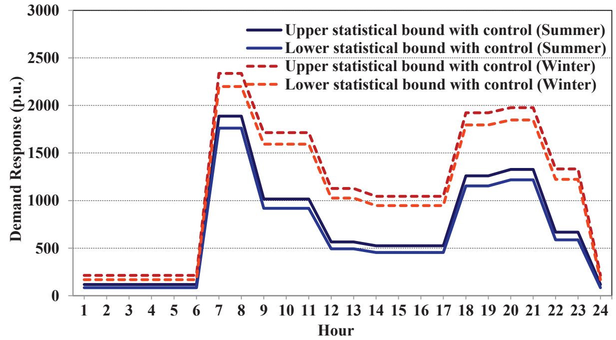

Figure 11: 90% confidence bounds on hourly demand response capacity from 10 000 EWHs with control over users' comfort in typical summer and winter days ($T_0 = 113°\mathrm{F}$)

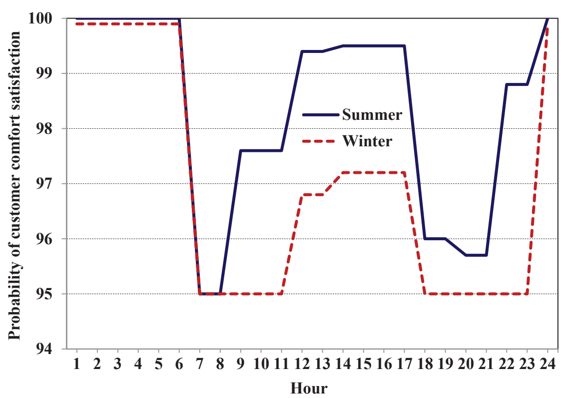

Figure 12: Metric C with control over users' comfort ($T_0 = 113°\mathrm{F}$)

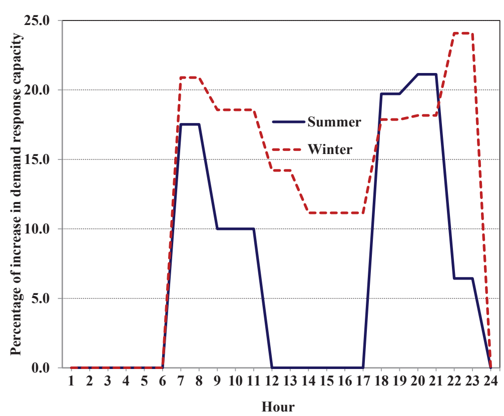

Figure 13: Percentage increase in the demand response capacity by reducing EWH users' comfort threshold from $T_0 = 115°\mathrm{F}$ to $T_0 = 113°\mathrm{F}$

comparing the results presented in Figures 8 and 11, the percentage of the increase in the demand response capacity is obtained and plotted in Figure 13.

Figure 13 indicates that the EWH users' comfort threshold may have preeminent impact on the available demand response capacity especially at hours with high demand for hot water.

5 Conclusion

This paper demonstrated the ability of the analytical approach and the control strategy introduced in Part I to leverage the aggregate demand of a large population of electric water heaters for the provision of sporadic use reserve capacity. The methodology developed in this two-part paper is essential to demand response aggregators in assessing available response capacity and its uncertainty while ensuring their responsive TCL users remain satisfied.

The validity of the proposed analytical models is investigated and verified using a physically-based model and through Monte Carlo simulations. Further, the trade-off between demand response capacity and EWH users' comfort satisfaction is investigated through several case studies. It is discovered that the existing trade-off between demand response capacity and EWH users' comfort satisfaction can be adjusted by constraining the on-time of EWHs in the population. Constraining the on-time guarantees some minimal users' comfort satisfaction during demand response calls, though this comes at the cost of decreasing demand response capacity. The numerical studies indicate that the minimum on-time control parameter T_{min}^{on} has an important role in satisfying the EWH users' comfort. Further, it has been observed that the optimal value of T_{min}^{on} is time dependent and changes over a daily cycle. Among important areas of future research is the extension of the proposed models and analytics to other TCLs such as air conditioners and fridges. Moreover, it would be desirable to assess the value of the approach in combination with online data collection from either smart meters or appliances.

A EWH data

The parameters of a typical EWH and the parameters of the hot water drawage beta distribution are given in Tables 4 and 5 respectively. Further, the parameters of the hot water drawage beta distribution for a daily cycle are provided in Table 6.

Table 4: Parameters of Typical EWH [2]

Parameter	Value
Volume (V)	50 gal (0.1893 m^3)
Max. thermostat deadband (T_{th}^{max})	135°F (57.2°C)
Min. thermostat deadband (T_{th}^{min})	115°F (46.1°C)
Inlet water temperature (T_{in})	60°F (15.5°C)
Rated power (P_r)	4.5 kW

Table 5: Hot Water Drawage Beta Distribution Parameters

Parameter	Value
Max. hot water drawage (L_d^{max})	25 gal (0.0947 m^3)
Min. hot water drawage (L_d^{min})	0 gal (0 m^3)
Shape parameter (p)	2
Shape parameter (q)	8
Hot water drawage mean (μ_{L_d})	5 gal (0.0189 m^3)

Table 6: Beta Distribution Parameters to Model Daily Hot Water Drawage

Hour	1	2	3	4	5	6	7	8
p	1	1	1	1	1	1	2	2
q	61.5	61.5	61.5	61.5	61.5	61.5	5.5	5.5
μ_{L_d}	0.4	0.4	0.4	0.4	0.4	0.4	6.7	6.7
Hour	9	10	11	12	13	14	15	16
p	1.8	1.8	1.8	1.7	1.7	1.6	1.6	1.6
q	10.5	10.5	10.5	17.5	17.5	17.5	17.5	17.5
μ_{L_d}	3.7	3.7	3.7	2.2	2.2	2.1	2.1	2.1
Hour	17	18	19	20	21	22	23	24
p	1.6	2	2	2	2	2	2	1
q	17.5	10	10	9.5	9.5	19	19	61.5
μ_{L_d}	2.1	4.2	4.2	4.4	4.4	2.4	2.4	0.4

References

[1] A. Abiri-Jahromi and F. Bouffard, Contingency-type reserve leveraged through aggregated thermostatically-controlled loads–part I: characterization and control,"submitted to IEEE Trans. Power Syst..

[2] J. Kondoh, N. Lu, and D.J. Hammerstrom, An evaluation of the water heater load potential for providing regulation service, IEEE Trans. Power Syst., 26(3), 1309–1316, Aug. 2011.

[3] D.S. Callaway, Tapping the energy storage potential in electric loads to deliver load following and regulation, with application to wind energy, Energy Conv. Manag., 50(5), 1389–1400, May 2009.

[4] C. Forbes, M. Evans, N. Hastings and B. Peacock, Statistical Distributions, New York, NY: Wiley, 2010.

[5] M. Dong, P.C.M. Meira, W. Xu, and C.Y. Chung, Non-Intrusive Signature Extraction for Major Residential Loads, IEEE Trans. Smart Grid, 4(3), 1421–1430, Sep. 2013.

[6] A. Papoulis, Probability, Random Variables, and Stochastic Processes, 3rd ed., New York, NY: McGraw-Hill, 1991.

[7] J.A. Short, D.G. Infield, and L.L. Ferris, Stabilization of grid frequency through dynamic demand control, IEEE Trans. Power Syst., 23(3), 1284–1293, Aug. 2007.

[8] A. Molina-García, F. Bouffard, and D.S. Kirschen, Decentralized demand-side contribution to primary frequency control, IEEE Trans. Power Syst., 26(1), 411–419, Feb. 2011.